Proceedings of the
Annual Stability Conference
Structural Stability Research Council
Charlotte, North Carolina, April 11-14, 2023

The impact of valency and the orientation of the members on the global stability of lattice steel domes

Ranjith Kolakkattil[1], Konstantinos Daniel Tsavdaridis[2], Arul Jayachandran Sanjeevi[3]

Abstract

Different single-layer lattice domes are created based on varying the arrangement of members. Although the stability of triangulated lattice domes has been studied earlier, the influence of the arrangement of members on their stability has not been investigated. The arrangement of members in lattice structures can be redefined based on the valency of different elements and the orientation of the members. Valency gives the interconnection between different elements, and orientation provides the spatial arrangement of the member with respect to the circumferential and radial directions. The variation of these two factors fundamentally defines the overall stability of single-layer lattice domes. Therefore, the influence of the valency and orientation of members on the stability of single-layer lattice domes is studied in this paper by comparing the elasto-plastic stability of commonly adopted single-layer lattice dome configurations, such as Kiewitt, Schwedler, Lamella, Radial rib, Sunflower, and Hexagon domes. The geometrical and material non-linear analyses of the selected single-layer domes reveal that the higher edge valency of vertices, higher vertex valency of cells, and the members oriented along the radial and circumferential directions increase the overall stability of the structure. These results help to identify the optimum number and orientation of the members at each node of the structure so that designers can adopt new configurations with higher stability and load capacity.

1. Introduction

Reticulated steel domes are constructed to cover large column-free areas with maximum volume enclosures, such as the roofs of coal storage yards, petroleum storage tanks, and indoor stadiums. The major advantage of dome structures is their ability to resist external loads through their shape or geometry, making them more efficient than other structural forms such as frame structures and space grids. They are lighter structures compared to other forms, as external loading is resisted by axial forces developed in the members (Makowski 1986). When a structure is lighter and the number of intermittent supports is at a minimum, stability is a concern for design engineers. The failure of dome structures in the past has indicated that the chance of

[1] PhD Candidate, Department of Civil Engineering, Indian Institute of Technology Madras, Chennai, India <ranjithk@alumni.iitm.ac.in>
[2] Professor, Department of Civil Engineering, School of Mathematics, Computer Science and Engineering, City University of London, United Kingdom <konstantinos.tsavdaridis@city.ac.uk>
[3] Professor, Department of Civil Engineering, Indian Institute of Technology Madras, Chennai, India <aruls@civil.iitm.ac.in>

instability—such as the occurrence of snap-through buckling—is very high for reticulated dome structures, especially single-layer reticulated dome configurations (Levy and Salvadori 2002). As single-layer dome structures consist of members and connections, the slenderness of the members and the rigidity of the connections play a significant role in their local and global stability (IASS 2014).

The stability investigations on reticulated structures mainly focused on local instability, global instability, and their interaction. The instability behavior in reticulated structures depends on geometrical factors and behavioral factors (Gioncu and Balut 1992). The geometrical factors include shell geometry and mesh density, while the behavioral factors include different types of nonlinearity, instability forms, imperfections, stiffness of the joint, and external load distribution. The studies on stability of dome structures focused mainly on behavioral factors, where the effect of additional parameters, such as the depth of the dome and support conditions, were also investigated.

Earlier, the stability of reticulated shells was investigated based on equivalent shell analysis (Wright 1965; Suzuki et al. 1992; and Dulacska and Kollar 2000). The comparison of buckling of reticulated shells based on equivalent shell analysis and discrete analysis showed the superiority of discrete analysis over equivalent shell analysis (Forman and Hutchinson 1970). Later, most of the studies were based on discrete analysis due to the accurate and faster analysis possible with the help of computers. Instability analysis based on the tangent stiffness matrix method found that the instability of a single member can affect the global stability of the spatial structures (Tanaka et al. 1985). The slenderness of the member will cause the member to buckle, which can initiate global buckling in reticulated structures (Lenza 1992). Progressive collapse analysis of dome structures revealed that dynamic propagation of snap-through buckling can also result in the overall collapse of reticulated dome structures (Abedi and Parke 1996). Therefore, local stability is critical for the overall stability of light structures such as reticulated domes. Many studies on local stability were conducted to identify the effect of local instability on the overall performance of reticulated structures (Gioncu 1995; Yang et al. 1996; Fan et al. 2010; and Fan et al. 2012). Global stability investigations of reticulated structures revealed the significance of joint rigidity, asymmetric load distributions, rise-to-span ratio, non-linearity, and imperfections. The experimental and numerical study of single-layer reticulated domes with semi-rigid joints found the effect of rigidity of connections on the global stability of dome structures (Lopez et al. 2007 and Ma et al. 2015). The rigidity of the joints can also influence the optimization of grid structures with semi-rigid joints (Tsavdaridis et al. 2020). The recent studies based on numerical analysis included different parameters such as rise-to-span ratio, initial curvature of the members, and the effect of load distributions (Fan et al. 2010; Fan et al. 2012; and Yan et al. 2016).

The majority of the investigations were on triangulated single-layer domes, as triangulated domes provide the most stable structure. However, the effect of member arrangement on the stability and performance of reticulated domes is limited. The comparison of member arrangement in single-layer cylindrical shells was conducted earlier (Sheikh 2001; Sheikh 2002; and Kolakkattil et al. 2022a). The parameters defined by Loeb (2012)—dimensionality, valency, and extent—can be introduced in the configuration of single-layer dome configurations (Kolakkattil et al. 2022b). The investigation based on the edge valency on the stability of three single-layer steel dome configurations revealed the effect of higher edge valency of vertices and lower edge valency of faces on the buckling load of latticed domes (Kolakkattil et al. 2022c). As many dome configurations can be created based on varying the defined parameters, the effect of member arrangement on global stability can be studied by considering different configurations that are commonly adopted. In addition to the member arrangement, the orientation of the members also plays a crucial role in the stability and overall load capacity of single-layer reticulated dome structures. Therefore, this study primarily investigates the effect of the edge valency of vertices, the vertex valency of cells, and the orientation of the members on the stability of usually adopted single-layer dome configurations.

In the initial stage of the study, different configurations were selected and subjected to buckling analysis and nonlinear analysis to obtain the optimum parameters. The variation of load capacity, by keeping total weight and total sectors equal among all configurations, was examined to find the efficient configuration. The effect of member orientation is investigated by varying the face valency in the final stage. The above comparison of different configurations will help to find the optimum member arrangement in a dome structure so that the load capacity can be improved without affecting the overall cost.

2. Single-layer dome configurations based on parameterization

Different dome configurations can be created on the basis of parameterization principles. The basic factors that constitute any spatial structure are form, internal structure, and connections (IASS 1984). The form provides the overall shape for the spatial structure. The spherical domes are an example of these forms. Internal structure refers to the internal arrangement of members in a spatial structure. Connections refer to the joining system used to connect the members in the internal structure. The global and local stability of any spatial structure depends on these three factors (Fig. 1). This paper discusses the effect of internal structures on the stability of single-layer reticulated steel domes.

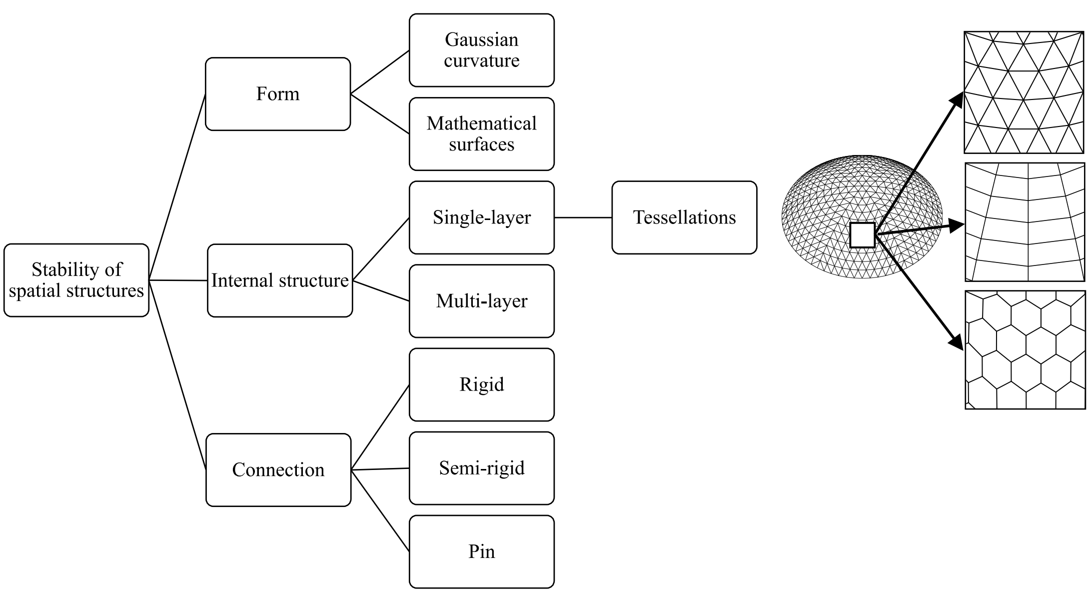

Figure 1: The basic features affecting the stability of spatial structures are form, internal structure, and connections. The present investigation studies the influence of member arrangement on the stability of single-layer lattice domes.

2.1 Internal structure in a dome configuration

The internal structure of single-layer domes consists of members arranged in different ways on a curved surface. The spherical surface is used as the surface of revolution in most of the commonly adopted dome structures. The popular single-layer reticulated dome configurations based on the different arrangements of members are provided in Fig. 2. The method used to create these dome configurations includes the selection of a curved surface (spherical surface is adopted for the single-layer lattice domes provided in Fig. 2) and arranging the members on the surface. Similarly, an elliptic or parabolic surface will result in a different dome configuration. The stability and overall performance of single-layer dome configurations subjected to external loads vary depending on the arrangement of the members. In order to understand how member arrangement affects the stability of the single-layer dome configurations, the basic difference between the member arrangements should be identified with the help of unique parameters. The parameters defined for any structure—dimensionality, valency, and extent (Loeb 2012)—can be introduced to distinguish between dome structures based on the arrangement of members.

Any internal structure of a spatial structure can be defined as the combination of elements such as vertices, edges, faces, and cells. The interrelationship between these elements can be defined on the basis of the three parameters (i.e., dimensionality, valency, and extent). Dimensionality specifies the degrees of freedom of an element. The dimensionality of a vertex is zero, and the dimensionality of an edge is one (Fig. 3). Valency defines the number of elements of a unique dimensionality that connect to an element of a different dimensionality (Loeb 2012). For example, the edge valency of a vertex in the Kiewitt dome configuration (Fig. 2(a)) is six as it is connected to six edges. Similarly, a three-dimensional structure, such as a dome, can have different valencies so that the entire interconnection between the members can be defined (Fig. 3). The third parameter, extent, defines the magnitude of each element. For example, the extent of an element with dimensionality one (i.e., edges) is length, and the extent of an element with dimensionality two (i.e., faces) is area. The extent indirectly provides the properties of elements such as the slenderness of the member and total material utilization. The given three parameters help to identify different configurations (Kolakkattil et al. 2022b) and study the effect of member arrangement on the overall stability and load capacity of single-layer reticulated domes.

In addition to the valency of the elements, the orientation of the members plays a critical role in the stability of the reticulated shells. Although valency and other parameters are the same for two reticulated shells, different orientations of the members can result in different behavior when subjected to external loading. For example, consider the Radial rib dome (Fig. 2(e)) and Lamella dome (Fig. 2(f)). The edge valency and face valency of both configurations are the same. However, the eigenvalue buckling analysis of the two dome configurations shows that the first buckling mode is different for both structures (Fig. 4), which signifies the importance of considering member orientation, in addition to the parameters that have been discussed earlier. Therefore, the selected dome configurations with different parameters (Fig. 2) were subjected to Geometrical Material Nonlinear Analysis (GMNA) to understand the combined effect of the defined parameters and the orientation of the members.

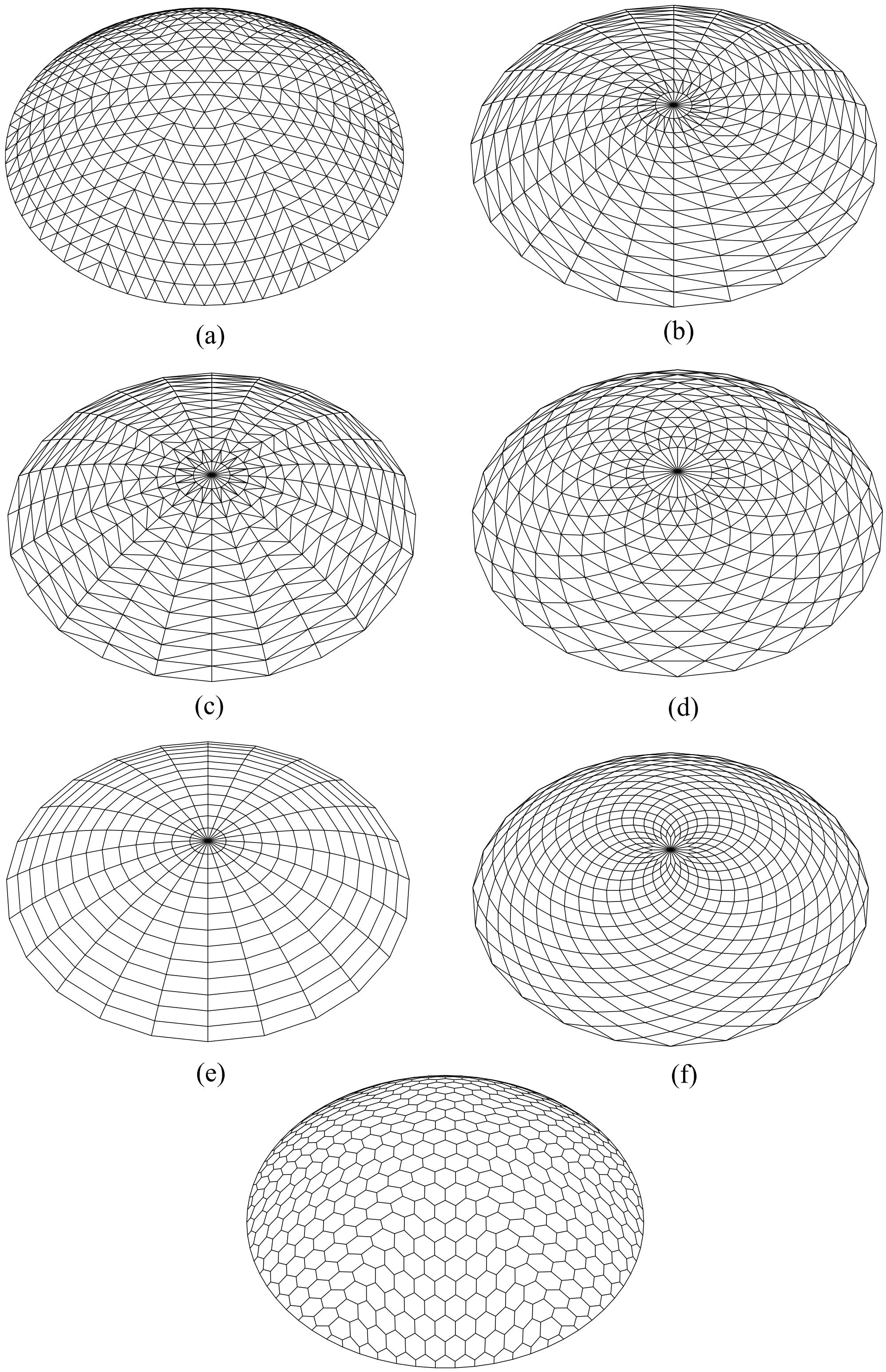

Figure 2: Single-layer dome configurations on the basis of variations in the defined parameters: (a) Kiewitt - 6 dome (b) Schwedler monoclinal dome (c) Schwedler bidirectional dome (d) Sunflower dome (e) Radial rib dome (f) Lamella dome (g) Hexagon dome

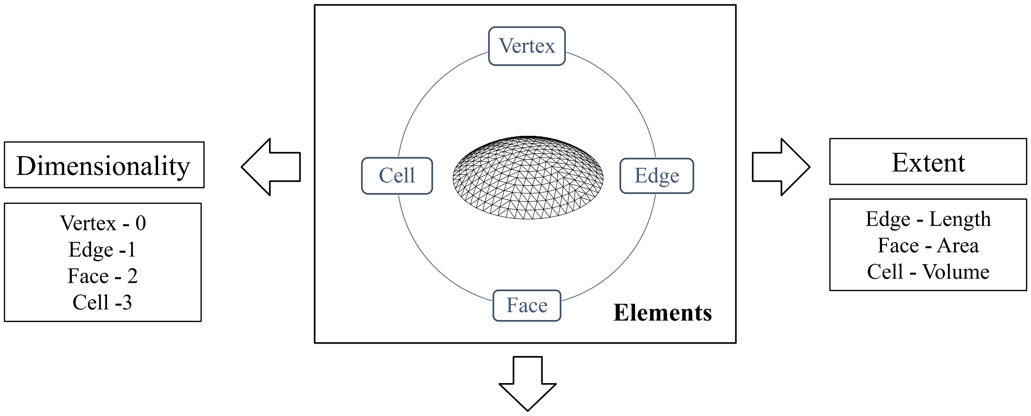

Valency

Element	Vertex Valency	Edge Valency	Face Valency	Cell Valency
Vertex	-	V_1	V_2	V_3
Edge	2	-	E_2	E_3
Face	F_0	F_1	-	2
Cell	C_0	C_1	C_2	-

Figure 3: The representation of three parameters used to identify a dome configuration. Parameters—dimensionality, valency, and extent—provide the relationship between different elements (vertices, edges, faces, and cells).

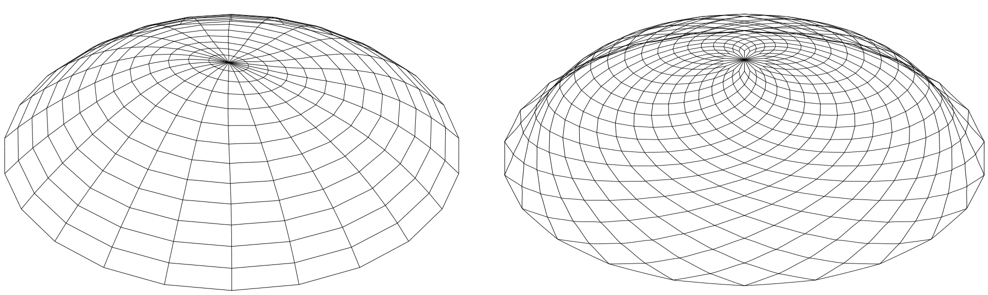

(a) (b)

Figure 4: First buckling mode is different for the configurations even though the edge valencies are the same, indicating the influence of member orientation on global stability: (a) Radial rib dome (b) Lamella dome

2.2 Numerical analysis

The single-layer dome configurations were generated by varying the defined parameters with the help of Formex Algebra (Nooshin and Disney 2001). Finite element models were created in Abaqus to perform the eigenvalue buckling analysis and nonlinear analysis. The members were modeled with element ‘B32’ (three-noded beam element), and the connections between the members were modeled as rigid. Each member was subdivided into four elements. The span of the dome configuration was fixed at 40 meters, and the rise-to-span ratio was fixed at 1:5. The supports were modeled as pin joints. Circular hollow cross-sections with diameter of 89 mm and thickness of 4 mm (CHS 80) were adopted for all the members based on the design guidelines from IS 800-2007. Elasto-perfectly plastic constitutive relation was used for the steel member sections, with Young's modulus of 200 GPa and Yield stress of 310 MPa. Initially, eigenvalue buckling analysis was performed to find the buckling mode and the lowest load factor. Subsequently, Geometrically and Materially Nonlinear Analysis (GMNA) was performed to identify the load capacity for the selected dome configurations subjected to uniform gravity load. The limit load was calculated for all configurations based on the Riks method.

When the type of configuration changes, the total length of the members and the total weight of the steel used in the configuration also change. Therefore, configurations were created such that the total length of the members was nearly the same in the initial analysis. Different properties of the dome configuration, such as total vertices, edges, extent, and load capacity, were compared for the selected configurations (Fig. 5). The results show that the Kiewit-6 dome configuration has the higher load capacity, the minimum number of edges, and a small variation in the extent. Therefore, the analysis clearly shows the reason for the high popularity of the Kiewitt-6 dome among designers compared to other single-layer dome configurations. The Lamella dome was found to have the lowest buckling load capacity among the selected configurations. The variation of extent among the edges was higher for all configurations except Kiewitt-6 and Hexagon dome. Although the edge valency of vertices was high for the Lamella dome compared to the Hexagon dome, the load capacity of the Hexagon dome was much higher (nearly ten times) than the load capacity obtained for the Lamella dome. Both dome configurations do not have radial members or ring members. Lamella domes have only diagonal members, and Hexagon domes have members with a smaller extent. The results obtained from the analysis show that the orientation of the member plays a significant role in addition to the basic parameters such as valency.

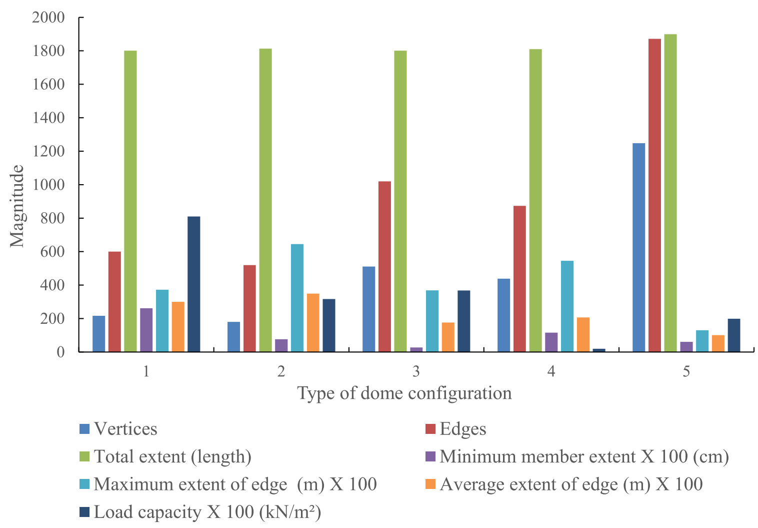

Figure 5: Variation of different properties of the dome configurations when the total member extent used was similar: (1) Kiewitt-6 dome (2) Schwedler dome (3) Radial rib dome (4) Lamella dome (5) Hexagon dome. The rise-to-span ratio of the dome configurations is 1:5.

When the configurations with the same extent (or weight) were subjected to the analysis, the slenderness of the members near the support region was very high for configurations with radial members (i.e., Radial rib dome and Schwedler dome), due to the usage of the same member cross-section (i.e., CHS 80) throughout the configuration (Fig. 6). Therefore, the member extent was restricted—by keeping the same face valency for all the configurations—to identify the effect of member orientation on the buckling load capacity. The same face valency is obtained in dome configurations by fixing the number of faces along the radial direction (N) and the number of faces along the circumferential direction (M) with the help of the Formex Algebra (Fig. 7). The properties of the new dome configurations are provided in Table 1. As the total weight of the structure varied with each configuration, a parameter was introduced, after the nonlinear analysis, to incorporate the effect of the total weight of the structure (Eq. 1).

$$\lambda = \frac{P}{w} \tag{1}$$

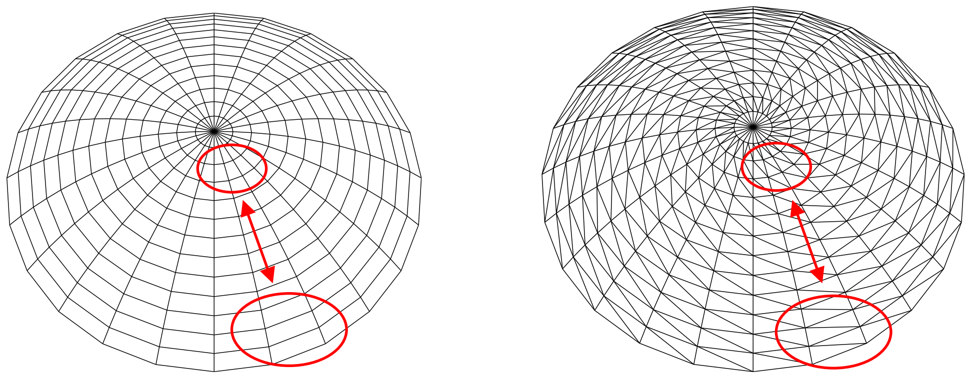

(a) (b)

Figure 6: Variation of member length from apex to support for dome configurations with radial members: (a) Radial rib dome (b) Shwedler monoclinal dome

Table 1: The properties of the selected configurations along with the values of M and N

Dome configuration	M	N	Vertices	Edges	Extent for length (m)	Minimum extent (m)	Maximum extent (m)	Average extent (m)
Kiewitt-6 dome	12	6	469	1332	2674.08	1.74	2.53	2.008
Schwedler-monoclinal	12	24	313	912	2453.93	0.443	5.33	2.69
Schwedler-bidirectional	12	24	313	912	2453.93	0.443	5.33	2.69
Radial Rib dome	12	24	313	624	1448.808	0.443	5.22	2.322
Lamella dome	12	24	601	1200	2182.37	0.891	5.22	1.819
Sunflower	12	24	313	912	2359.464	0.821	5.22	2.587
Hexagon dome	12	6	936	1404	1625.604	0.614	1.74	1.158

Here, P is the load capacity (kN/m^2), and w is the total weight of the dome configuration. As the members were welded to each other, only the weight of the members was considered in the calculation. Initially, the variation of the parameter λ was compared with the edge valency of the vertices of the configurations. As the edge valency of the vertices was different at the support regions from that at the interior regions of a dome configuration (Fig. 8), the average edge valency of vertices was considered to incorporate the effect of edge valency at the support (Eq. 2). Here, $\overline{V_1}$ represents the average edge valency of the vertices, N_0^r represents the number of vertices for which the edge valency is 'r', and N_0 is the number of vertices. For the given configurations with a span of 40 meters, the average edge valency of vertices is given in Table 2.

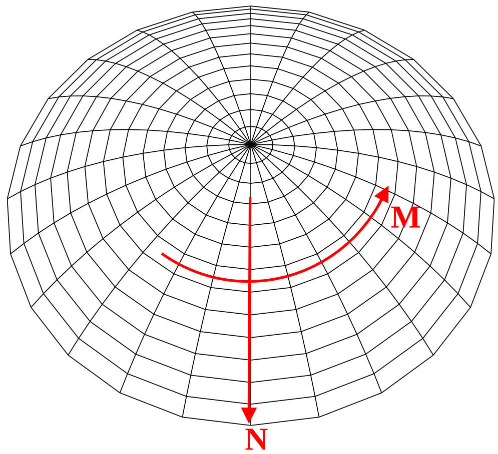

Figure 7: Variation in the number of faces was obtained by changing the two parameters: the number of faces along the radial direction (N) and the number of faces along the circumferential direction (M).

$$\bar{V}_1 = \sum_{r=2}^{n} \frac{rN_0^r}{N_0} \tag{2}$$

The first buckling mode shape based on eigenvalue buckling analysis changes with the type of configuration (Fig. 9), showing the influence of edge valency and orientation of members on the behavior of single-layer dome configurations under gravity loading.

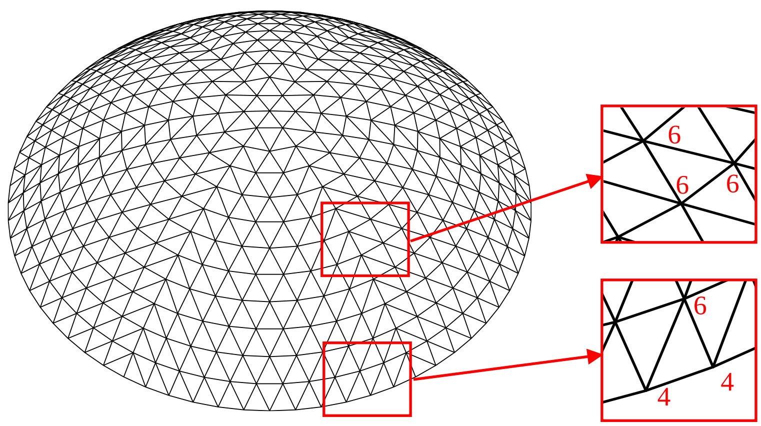

Figure 8: The change in edge valency of the vertex at the support region from the interior region

Table 2: Average edge valency of vertices for the dome configurations

Dome configuration	Average edge valency of vertex
Kiewitt-6 dome	5.69
Schwedler-monoclinal	5.83
Schwedler-bidirectional	5.827
Radial Rib dome	3.99
Lamella dome	4
Sunflower dome	5.827
Hexagon dome	3

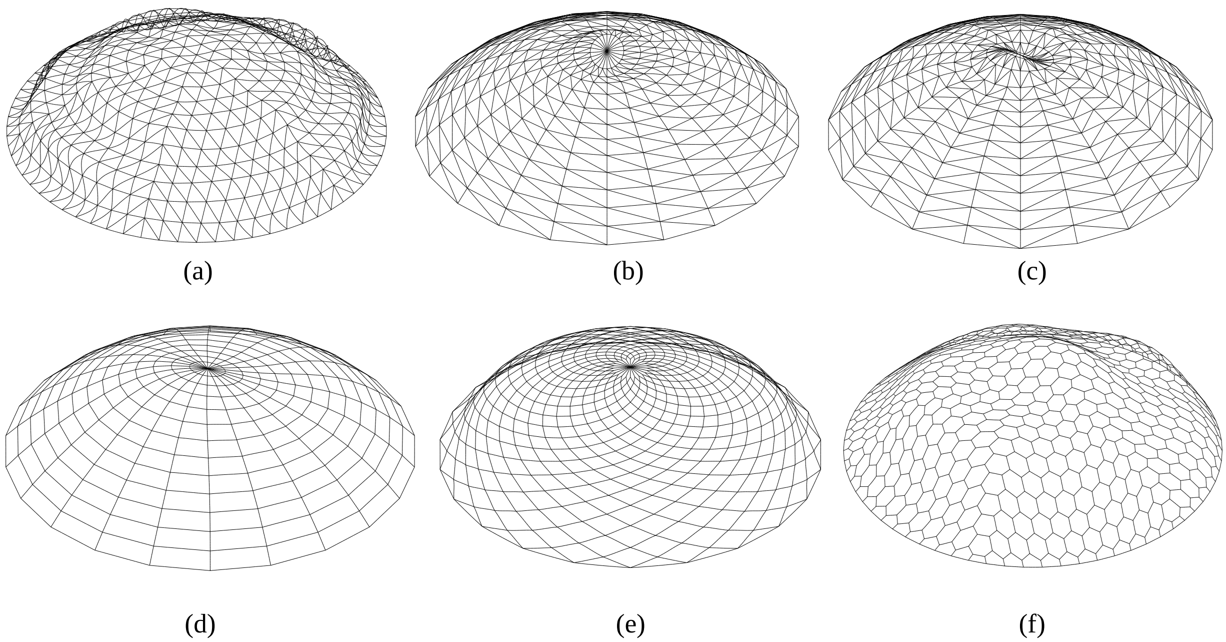

Figure 9: First buckling mode for the dome configurations: (a) Kiewitt dome (b) Schwedler monoclinal dome (c) Schwedler bidirectional dome (d) Radial rib dome (e) Lamella dome (f) Hexagon dome

The variation of the limit load with the average edge valency of vertices shows the higher buckling load capacity of reticulated domes with higher edge valency (Fig. 10). However, the Lamella dome, which has a higher average edge valency, has a lower load capacity compared to the Hexagon dome. Similarly, the value of λ is higher for the Radial rib dome compared to triangulated domes other than the Kiewitt dome (i.e., Schwedler domes and Sunflower dome), whereas the average value of edge valency of vertices is higher for triangulated domes compared to the Radial rib dome. These observations signify the influence of member orientation (especially radial members) and face valency on the overall performance of single-layer dome configurations. In addition to that, the value of the parameter λ was higher for the Kiewitt dome among all the triangulated shell configurations, even though all the triangulated dome configurations had nearly the same edge valency. Therefore, the orientation of the members plays a significant role in the stability and load capacity of single-layer reticulated shell configurations.

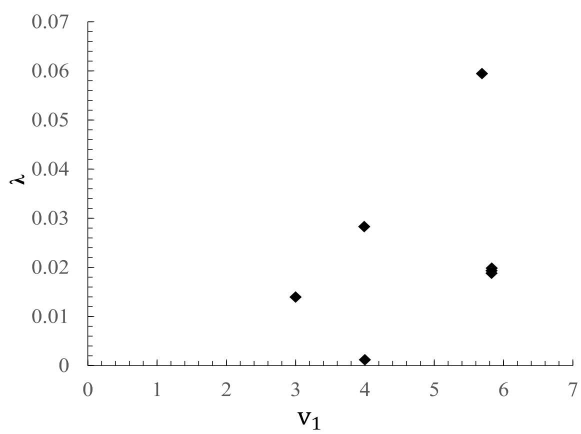

Figure 10: The variation of the parameter λ with average edge valency of vertices

In order to achieve different face valencies, the number of faces along the radial direction (N) was fixed (i.e., N = 12) and the number of faces along the circumferential direction (M) was varied. The change in buckling load was analyzed with the variation in the value of M for different configurations. All the properties of the dome structures and the analysis procedure were the same as in the previous analysis.

The first eigenvalue based on the buckling analysis of the Kiewitt dome with different M values (M = 4, 5, 6, 7, and 8) was calculated. In order to incorporate the effect of the total weight of the structure, a parameter α was introduced similar to Eq. 1 by taking the ratio of the first eigenvalue to the total weight of the structure (w). The variation in the value of α with the value of M is shown in Fig. 11 for the Kiewitt dome with the rise-to-span ratio of 0.2. The value of α increases with the value of M and decreases after reaching the maximum value at M = 7, which signifies the importance of face valency in deciding the dome configuration with the optimum buckling load. Kiewitt-6 (Kiewitt dome with M = 6) and Kiewitt-8 (Kiewitt dome with M = 8) are the most commonly adopted dome configurations due to their efficiency. However, Kiewitt-7 (Kiewitt dome with M = 7) was found to have better performance when comparing the total weight of these structures. The first buckling mode of all Kiewitt domes with varying values of M is provided in Fig. 12. The buckling mode shape looks similar when the value of M increases. The increase in the value of α also reduces once the value of M increases and reaches the value of seven (Fig. 11), since the reduction in slenderness will reduce once the M value increases.

The nonlinear analysis (GMNA) of Kiewitt domes with varying values of M was performed in the next stage. As the number of vertices or the vertex valency of the dome structure changes corresponding to the change in the value of M, the variation of λ is plotted with the vertex valency of the dome configurations (Fig. 13). Similar to the comparison of the first eigenvalue (Fig. 10), the value of λ increases initially, then decreases after reaching an optimum value. Vertex valency in the range of 500 was found to have the maximum buckling load capacity for the Kiewitt dome. When the vertex valency of the cell increases after reaching the optimum value, the chance of node buckling in dome configurations increases. Therefore, the buckling load capacity was reduced even though the vertex valency and edge valency of the cells increase.

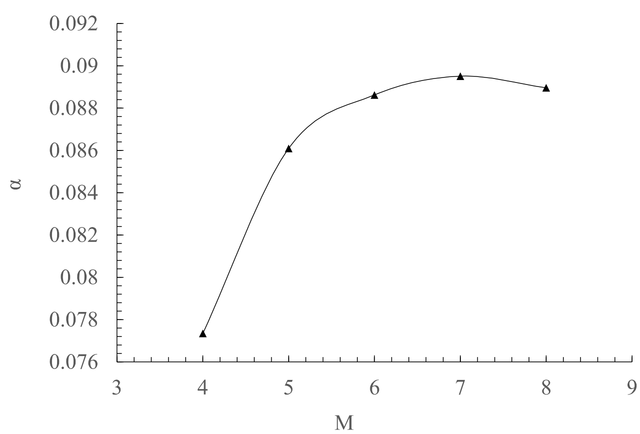

Figure 11: The variation of the parameter α with the value of M for the Kiewitt dome. The maximum value of α observed for M = 7.

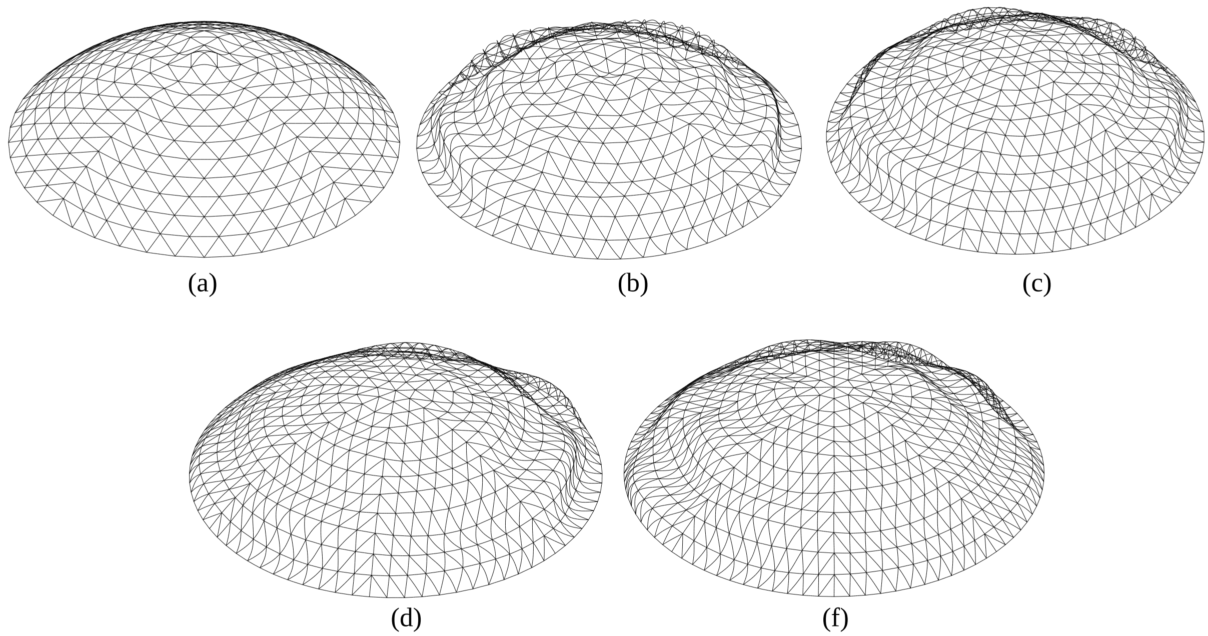

Figure 12: The first buckling mode shape for the Kiewitt dome with different face valency of the cell by varying the value of M: (a) M = 4 (b) M = 5 (c) M = 6 (d) M = 7 (e) M =8

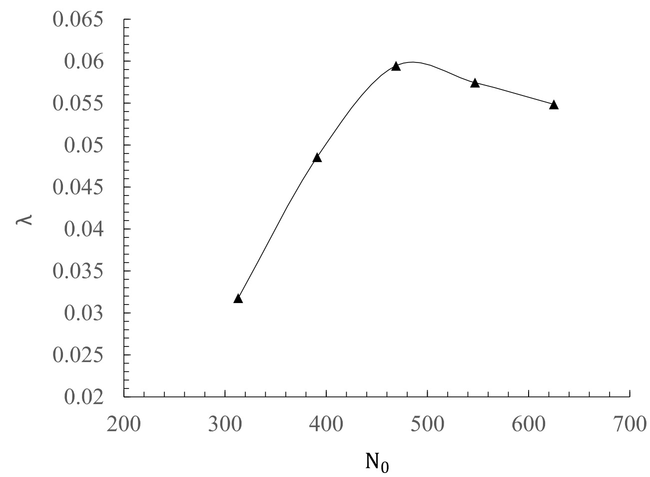

Figure 13: The variation of the parameter λ with the vertex valency of the cell for the Kiewitt dome

Similar to the nonlinear analysis conducted for the Kiewitt dome, the other dome configurations were subjected to GMNA to find the effect of valency and the orientation of the members on the stability and buckling load capacity. The results for the six dome configurations are given in Fig. 14. Similar to the results obtained for the Kewitt dome, all the configurations have a vertex valency of the cell where the maximum load capacity is obtained. The value of the λ increases initially and decreases after reaching the maximum value. There is a drastic reduction in the value of λ for the radial rib dome after reaching the maximum value. When the vertex valency of the cell reaches a value higher than the value corresponding to the maximum buckling load, the chance of node buckling increases, causing a reduction in the value of λ. The results also showed the significance of radial rib members and circumferential members in improving the stability and overall resistance of reticulated domes. These observations were specifically valid for

Shwedler and radial rib domes, where the vertex valency of the cell for reaching the maximum load capacity was lower compared to the dome configuration where only diagonal members were available (Lamella dome). For the Lamella dome, the vertex valency of the cell for obtaining the highest load capacity is more than 2000, which dome significantly increases the cost of the structure. Higher edge valency of vertices helps to increase the overall resistance for the Sunflower dome with lower vertex valency of the cell.

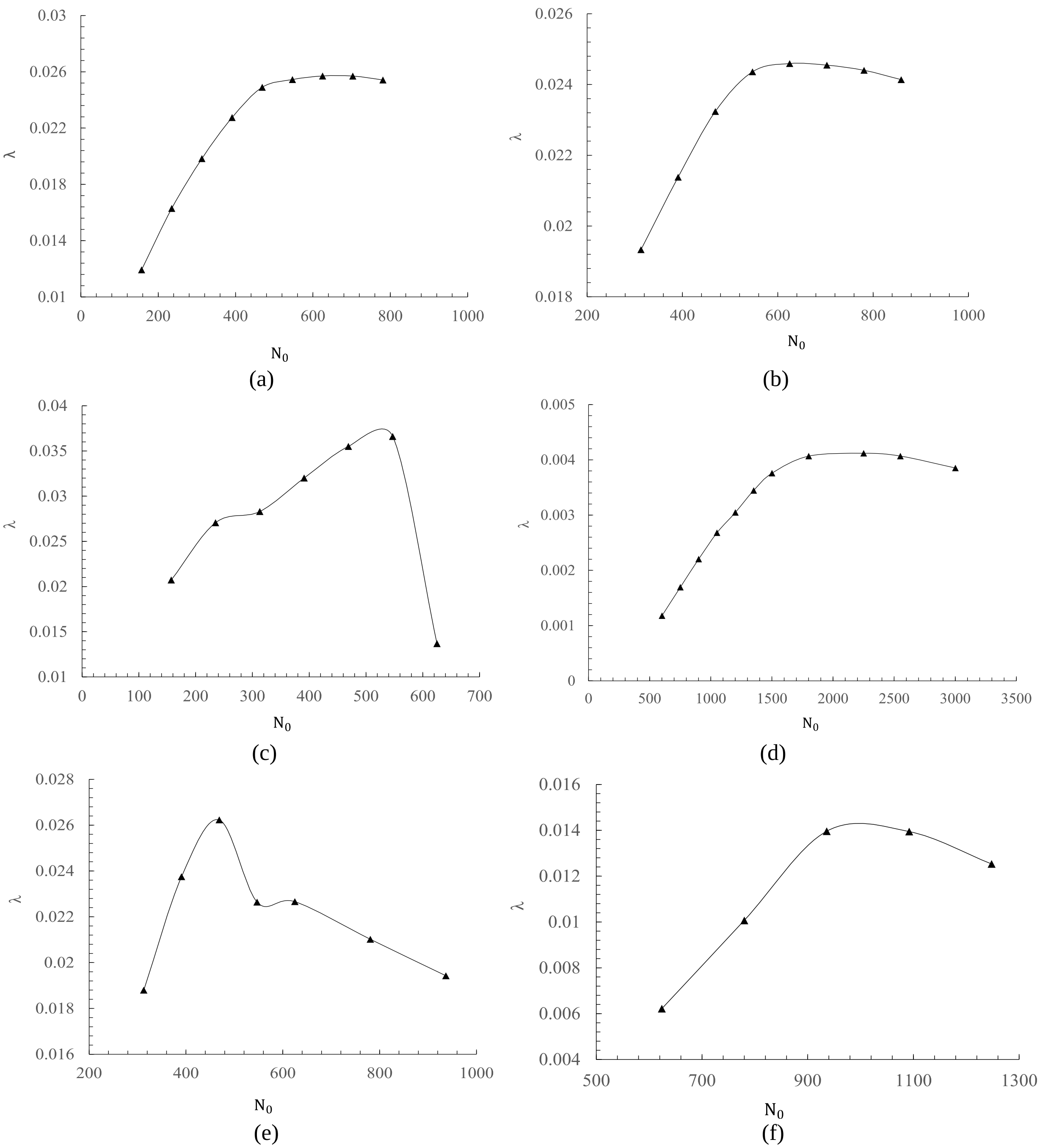

Figure 14: The variation of the parameter λ with the variation of N_0 : (a) Schwedler monoclinal dome (b) Schwedler bidirectional (c) Radial rib dome (d) lamella dome (e) Sunflower dome (f) Hexagon dome

3. Discussion

The valency of the elements and the orientation of the members plays a significant role in the stability and overall load resistance of single-layer reticulated domes. As the edge valency of the vertices increases, the load capacity and the overall stability of the dome configurations increases. Dome configurations with triangulation, where the edge valency of vertices is 6, were found to be efficient compared to other configurations with lower edge valency of vertices. The vertex valency of the cell, corresponding to the maximum load capacity, was lower for all the triangulated configurations as higher edge valency of vertices plays a significant role in resisting the external load. Among the triangulated dome configurations, Kiewitt dome was highly efficient with high load capacity, lower steel consumption, and lesser variation of member length. The orientation of the members, especially members in the radial directions helps to improve the stability, which is evident from the results obtained for the Radial rib dome and Schwedler dome. Even though the edge valency is lower, Radial rib domes have higher load capacity due to the presence of radial members.

The large variation in the length of circumferential members from apex to support is a concern with dome configurations with a high number of radial members (Fig. 6). When a large number of radial members are used, the apex is crowded with shorter members and the support region has members with large slenderness, which is not efficient. Hence, dome configurations with trimmed apex (less number of members at the top) could be adopted to increase efficiency. Further study on trimmed domes could help to understand the degree to which the members can be reduced at the apex region. The present study adopted a single span-to-rise ratio and a constant member cross-section for all the dome configurations. Further parametric study—with varying rise, span, member cross-sections, and support conditions—will help to validate the obtained results.

4. Concluding remarks

Commonly adopted single-layer domes were subjected to buckling analysis and geometrically and materially nonlinear analysis to identify the effect of valency and the orientation of the members. Initially, different configurations, with the same total extent for length, were configured and subjected to the analysis. Then, the buckling load of the configurations was calculated by keeping the valency of faces equal across the dome structures. Finally, the load capacity of different configurations with varying vertex valencies of the cell was found through the nonlinear analysis to identify the optimum parameters. The significant findings based on the study are the following:

- Kiewitt dome was found to be efficient, among the selected single-layer reticulated dome configurations, with a higher load capacity, a minimum number of connections, a minimum number of members, and a smaller variation in the length of the members across the structure.
- The buckling load increases with an increase in the edge valency of vertices for all the configurations. However, Lamella dome had a lower buckling load compared to the Hexagon dome, as the orientation of the members in the radial direction played a significant role in the overall resistance of the dome configurations.
- The load capacity increases with an increase in the vertex valency of the cell and reduces after reaching the peak value for all the configurations. The chance of node

buckling increases with the increase in the vertex valency of cells in all the configurations, which resulted in a reduction in the load capacity after reaching the maximum value.

- The face valency corresponding to the maximum load capacity was lower for dome configurations with higher edge valency of vertices. The face valency, for obtaining the maximum load capacity, was much high for configurations such as the Lamella dome due to the absence of radial rib members.
- The radial members had a significant role in the load transfer to the supports, and hence the presence of radial members increases the stability and overall resistance with lower steel consumption.

References

Abaqus CAE (2009). "Standard User's Manual", *Version 6.9*, Dassault Systemes Simulia.

Abedi, K., & Parke, G. A. R. (1996). "Progressive collapse of single-layer braced domes." *International Journal of Space Structures*, 11(3), 291-306.

Dulácska, E., & Kollár, L. (2000). "Buckling analysis of reticulated shells." *International Journal of Space Structures*, *15*(3), 195-203.

El-Sheikh, A. (2001). "Performance of single-layer barrel vaults with different configurations." International Journal of Space Structures, 16(2), 111-123.

El-Sheikh, A. (2002). "Effect of geometric imperfections on single-layer barrel vaults." International Journal of space structures, 17(4), 271-283.

Fan, F., Cao, Z., & Shen, S. (2010). "Elasto-plastic stability of single-layer reticulated shells." *Thin-Walled Structures*, 48(10-11), 827-836.

Fan, F., Yan, J., & Cao, Z. (2012). "Elasto-plastic stability of single-layer reticulated domes with initial curvature of members." *Thin-Walled Structures*, 60, 239-246.

Forman, S. E., & Hutchinson, J. W. (1970). "Buckling of reticulated shell structures." *International Journal of Solids and Structures*, 6(7), 909-932.

Gioncu, V. (1995). "Buckling of reticulated shells: state-of-the-art." *International Journal of Space Structures*, 10(1), 1-46.

Gioncu, V., & Balut, N. (1992). "Instability behaviour of single-layer reticulated shells." *International journal of space structures*, 7(4), 243-252.

IASS, WG 8. (2014). "Guide to Buckling Load Evaluation of Metal Reticulated Roof Structures (Report of Activities WG 8)." *International Association for Shell and Spatial Structures.*

IS 800 (2007). "General construction in steel-code of practice." 3rd Revision, *Bureau of Indian Standard*, New Delhi, India.

Kolakkattil, R., & Jayachandran, A. (2022). "Global Stability Behavior of Single-Layer Reticulated Domes Created Using a New Nomenclature." *Journal of the International Association for Shell and Spatial Structures,* 63(1), 31-48.

Kolakkattil, R., Tsavdaridis, K. D., & Sanjeevi, A. J. (2022). "Global stability of single-layer reticulated domes based on the valency of structural elements." In Proceedings of the Annual Stability Conference Structural Stability Research Council, Denver, Colorado, 720-734.

Kolakkattil, R., Tsavdaridis, K. D., & Sanjeevi, A. J. (2022). "The effect of edge valency on the load resistance of single-layer reticulated cylindrical shells." Journal of Constructional Steel Research, 198, 107531.

Lenza, P. (1992). "Instability of single layer doubly curved vaults." International Journal of Space Structures, 7(4), 253-264.

Lenza, P. (1992). "Instability of single layer doubly curved vaults*." International Journal of Space Structures*, 7(4), 253-264.

Levy, M., & Salvadori, M. (2002). *Why buildings fall down: How structures fail*. WW Norton & Company.

Loeb, A. (2012). *Space structures: Their harmony and counterpoint.* Springer Science & Business Media.

López, A., Puente, I., & Serna, M. A. (2007). "Numerical model and experimental tests on single-layer latticed domes with semi-rigid joints." *Computers & structures*, *85*(7-8), 360-374.

Ma, H., Fan, F., Wen, P., Zhang, H., & Shen, S. (2015). "Experimental and numerical studies on a single-layer cylindrical reticulated shell with semi-rigid joints." *Thin-Walled Structures*, *86,* 1-9.

Makowski, Z. S. (Ed.). (1986). *Analysis, design, and construction of braced barrel vaults.* CRC Press.
Nooshin, H., & Disney, P. (2000). "Formex configuration processing I." *International journal of space structures,* 15(1), 1-52.
Suzuki, T., Ogawa, T., & Ikarashi, K. (1992). "Elastic buckling analysis of rigidly jointed single-layer reticulated domes with random initial imperfection." *International Journal of Space Structures,* 7(4), 265-273.
Tanaka, K., Kondoh, K., & Atluri, S. N. (1985). "Instability analysis of space trusses using exact tangent-stiffness matrices." *Finite elements in analysis and design,* 1(4), 291-311.
Tsavdaridis, K. D., Feng, R., & Liu, F. (2020). "Shape Optimization of Assembled Single-Layer Grid Structure with Semi-Rigid Joints." *Procedia Manufacturing, 44,* 12-19.
WG 8. (1984). "Analysis, Design and Realization of Space Frames." *Bulletin of IASS, 84,* 96-406.
Wright, D. T. (1965). "Membrane forces and buckling in reticulated shells." *Journal of the structural division,* 91(1), 173-201.
Yan, J., Qin, F., Cao, Z., Fan, F., & Mo, Y. L. (2016). "Mechanism of coupled instability of single-layer reticulated domes." *Engineering Structures,* 114, 158-170.
Yang, Y. B., Yang, C. T., Chang, T. P., & Chang, P. K. (1997). "Effects of member buckling and yielding on ultimate strengths of space trusses." *Engineering Structures,* 19(2), 179-191.